Biosensors and Bioelectronics 29 (2011) 219–223

Contents lists available at ScienceDirect

Biosensors and Bioelectronics

journal homepage: www.elsevier.com/locate/bios

Short communication

Toxin detection by Si photosensitive biosensors with a new measurement scheme

Chan Woo Park*, Jong-Heon Yang, Chil Seong Ah, Chang-Geun Ahn, Yo Han Choi, Kwang Hyo Chung, Wan-Joong Kim, Gun Yong Sung

Biosensor Research Team, Electronics and Telecommunications Research Institute (ETRI), Daejeon 305-700, Republic of Korea

ARTICLE INFO

Article history:
Received 15 June 2011
Received in revised form 21 July 2011
Accepted 10 August 2011
Available online 18 August 2011

Keywords:
Photosensitive biosensor
CMOS compatible
Photodiode
Competitive assay
Mycotoxin

ABSTRACT

We propose a new type of photosensitive biosensor with a CMOS compatible Si photodiode integrated circuit, for the high-sensitive detection of small mycotoxin molecules requiring competitive assay approach. In this work, a photodiode is connected to the gate of a field effect transistor (FET) so that the open circuit voltage (V_{OC}) of the illuminated photodiode is transferred into the drain/source current (I_{DS}) of the FET. The sensing scheme employs competitive binding of toxin molecules (within the sample solution) and toxin–BSA conjugates (immobilized on the photodiode surface) with Au-nanoparticle-labeled antibodies, followed by silver enhancement to generate opaque structures on the photodiode surface. By utilizing the non-linear dependence of the V_{OC} on the light intensity, we can maintain a sufficiently high signal resolution at low toxin concentrations (with most of the incident light blocked) for the competitive assay. By monitoring the I_{DS} of the FET whose gate is driven by the V_{OC}, quantitative detection of Aflatoxin B1 has been achieved in the range of 0–15 ppb.

1. Introduction

The photosensitive biosensor employing metallic nanoparticle labels has been considered as a promising candidate for overcoming some drawbacks of conventional fluorescence-based methods (Ahn et al., 2010; Li et al., 2005; Wang et al., 2007). In this approach, metallic nanoparticles are hybridized with target molecules captured on a photodiode sensing area, and then enhanced further leading to screening of the incident light. The amount of target molecules can be monitored from the photoresponse in accordance with the opacity of the robust metal particle layer, which provides a more time-stable signal with no need for external optical excitation systems. As the output signal is fully electronic, large expensive optical reading instruments are not required and a miniaturized and integrated readout system can be constructed (Ahn et al., 2010; Li et al., 2005; Wang et al., 2007).

In previous works of photodiode biosensors (Ahn et al., 2010; Li et al., 2005; Wang et al., 2007), the coverage of metallic nanoparticles has been measured from the amount of photocurrent, which provided a high enough sensitivity to detect pM to nM range of proteins (Ahn et al., 2010) or DNA (Li et al., 2005; Wang et al., 2007) by sandwich assays. However, in the photocurrent-based approach, the overall level of photocurrent becomes too low near the full coverage of metal particles (where most of the incident light is blocked), which causes the degradation of signal resolution (Ahn et al., 2010).

On the other hand, in cases of detecting small molecules by competitive assays, the coverage of shadowing metal structures would be highest (darkest) at zero concentration, and then decreases as the target concentration increases. Therefore, for achieving highly sensitive and quantitative measurement of small molecules by photodiode sensors, an alternative sensing scheme is needed for enhancing the signal resolution at low concentrations.

In the present work, we propose a new type of photosensitive biosensor with a CMOS compatible Si photodiode integrated circuit, for the high-sensitive detection of small mycotoxin molecules. In this work, a photodiode is connected to the gate of a field effect transistor (FET) so that the open circuit voltage (V_{OC}) of the illuminated photodiode is transferred into the drain/source current (I_{DS}) of the FET. The sensing scheme employs competitive binding of toxin molecules (within the sample solution) and toxin–bovine serum albumin (BSA) conjugates (immobilized on the photodiode surface) with Au-nanoparticle-labeled antibodies, followed by silver enhancement to generate opaque structures on the photodiode surface. As the amount of toxin increases, less opaque becomes the photodiode surface resulting in a higher V_{OC}, where the V_{OC} increases non-linearly with the incident light intensity. By monitoring the channel current of the FET whose gate is driven by the V_{OC}, quantitative detection of Aflatoxin B1 has been achieved in the range of 0–15 ppb.

* Corresponding author. Tel.: +82 42 860 5249; fax: +82 42 860 6594.
E-mail addresses: chanwoo@etri.re.kr (C.W. Park), gysung@etri.re.kr (G.Y. Sung).

0956-5663/$ – see front matter © 2011 Elsevier B.V. All rights reserved.
doi:10.1016/j.bios.2011.08.009

2. Sensing scheme

Fig. 1a shows the cross-sectional structure and working principle of the sensor schematically. It was fabricated from a silicon-on-insulator (SOI) wafer with a p-type Si substrate, where an n-well was formed on the front surface to obtain an n+/n−/p−/p+ photodiode structure. A p-channel enhancement type FET (p-MOSFET) was fabricated on the SOI layer, with the gate being connected to the n-type side of the photodiode. When the photodiode is illuminated, a negative gate voltage (V_{OC} of the photodiode) is applied and the channel current increases. On the surface of the photodiode region, we immobilized toxin–BSA conjugates,

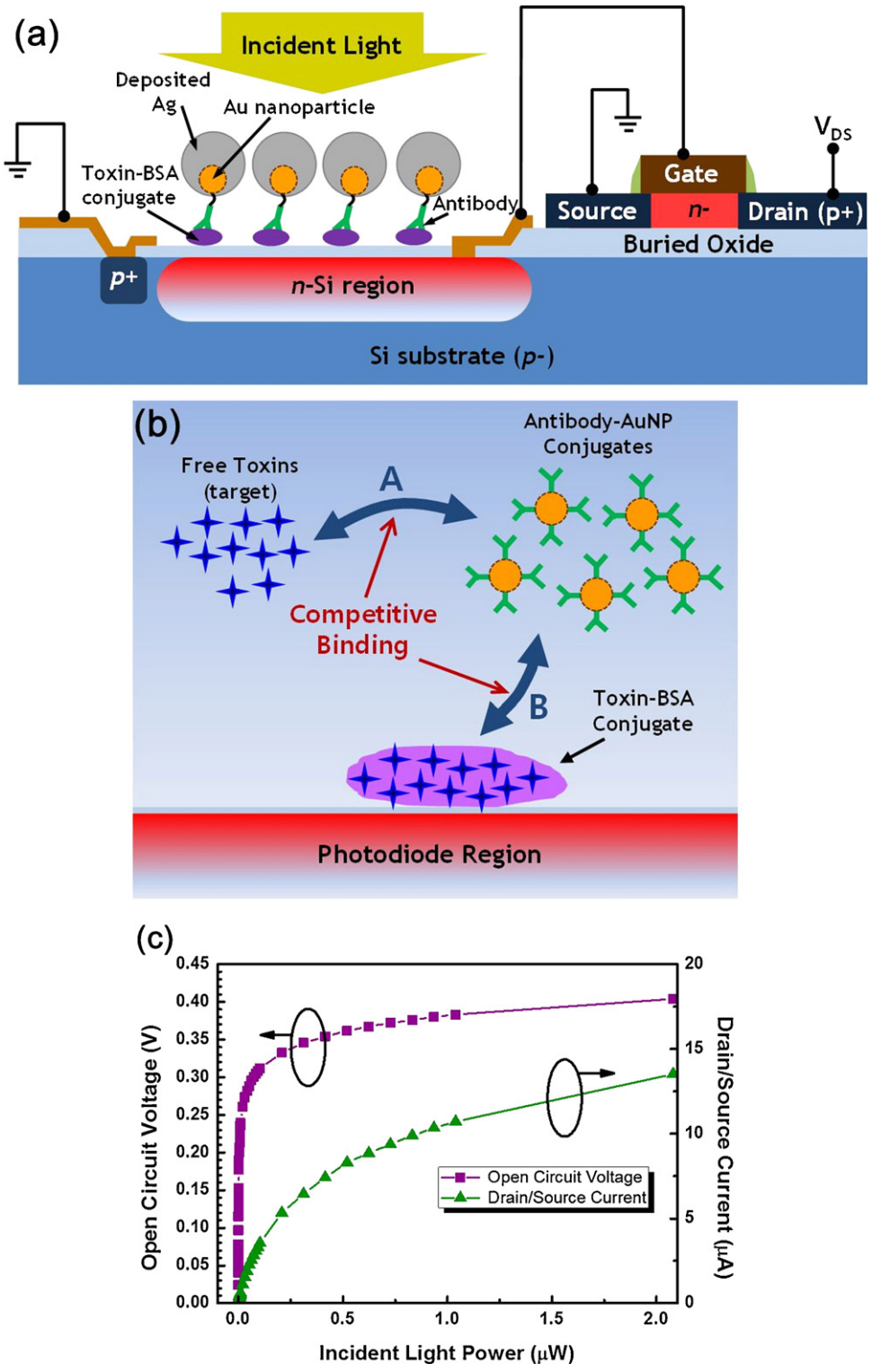

Fig. 1. (a) Schematic of the principle of toxin detection by the Si photodiode integrated circuit sensor. (b) Competitive binding of free toxin molecules (within the solution) and toxin–BSA conjugates (immobilized on the photodiode surface) with Au-nanoparticle-labeled antibodies. (c) Dependence of the open circuit voltage (V_{OC}) of a 300 μm × 300 μm Si photodiode and the drain/source current (I_{DS}) of a 0.5 μm p-MOSFET driven by the photodiode at a drain-source bias (V_{DS}) of 100 mV, on the incident light power.

which compete with free toxins (target) for binding with antibody-gold nanoparticle (AuNp) conjugates (Fig. 1b). The coverage of silver-enhanced AuNPs blocking the incident light decreases as the toxin concentration increases, leading to a larger I_{DS} of the FET.

3. Materials and methods

3.1. Fabrication of Si photosensitive biosensors

Photosensitive biosensors were fabricated from 8 in. SOI wafers with a 100-nm-thick top silicon layer (p-type, 8.5–22 Ω cm) and a 200-nm-thick buried oxide layer. First, the initial top Si layer was thinned down to 40 nm by dry oxidation and wet etching cycles, and then the active area for p-MOSFETs was defined by a local oxidation of silicon (LOCOS) process. During the LOCOS process, the whole thickness of the top Si layer outside the active region was oxidized. For forming photodiodes on the bottom p-type Si substrate, the oxide covering the photodiode region was removed by wet etching in a HF solution. Then, the exposed Si surface was sequentially implanted with 2.0e13 cm^{-2} and 5.0e15 cm^{-2} of phosphorus ions at 300 keV and 80 keV, respectively, followed by drive-in anneal at 1000 °C for 3 h. For forming p-MOSFETs on the top Si layer, the active area was implanted with 2.5e13 cm^{-2} of phosphorus ions at 25 keV, and then the gate oxide of 80 Å was grown. After patterning the poly-Si gate, the drain/source region was implanted with 2.0e15 cm^{-2} of boron ions at 40 keV, and rapid thermal annealed at 950 °C for 30 s. During the drain/source ion implantation, a p+ substrate contact for the photodiode was also formed. Finally, metal electrodes were formed as a stack of Au/Cr/Al (50 nm/5 nm/50 nm) by electron-beam evaporation and lift-off technique, followed by annealing at 400 °C for 30 min.

3.2. Immobilization of toxin–BSA conjugates on the Si photodiode surface

The Si photodiode surface was activated with hydroxyl (–OH) groups by low power oxygen plasma treatment (50 W, 5 min), and then functionalized with 3-aminopropyltriethoxysilane (APTES, Sigma–Aldrich) within a home-made Teflon reactor at 120 °C for 10 min. The amine-functionalized Si surface was immersed in a 25 wt% glutaraldehyde (Sigma–Aldrich) aqueous solution with 160 mM sodium cyanoborohydride ($NaBH_3CN$, Sigma–Aldrich) for 4 h, followed by rinsing with de-ionized water. During the reaction with glutaraldehyde, the amine-modified Si surface was functionalized with aldehyde groups. The immobilization of toxin–BSA conjugates was achieved by exposing the aldehyde-functionalized Si surface to 100 μg/ml of Aflatoxin B1–BSA conjugates (Sigma–Aldrich) in 10 mM phosphate buffer solution (pH 8.4) with 4 mM $NaBH_3CN$ for 12 h. Finally, the unreacted surface aldehyde was blocked with 1% casein in 10 mM phosphate buffer solution for 30 min.

3.3. Competitive immunoassay and enhancement of metallic nanoparticles

Immunogold conjugates were prepared by the conjugation of AuNPs (10 nm in diameter) with monoclonal antibodies of Aflatoxin B1 (SD Company, Korea) (Kim et al., 2007, 2010). Aflatoxin B1 (Sigma–Aldrich) molecules were dissolved in 70% methanol, and then diluted with 1× PBS solution (10 mM phosphate + 138 mM NaCl + 2.7 mM KCl, Sigma–Aldrich) at various concentrations of 0, 5, 10, and 15 ppb. The Aflatoxin B1–BSA conjugates-immobilized photodiode surface was incubated within the Aflatoxin B1 and immunogold conjugate solution for 1 h at 20 °C, followed by rinsing in 1× PBS several times. For further enhancement of captured

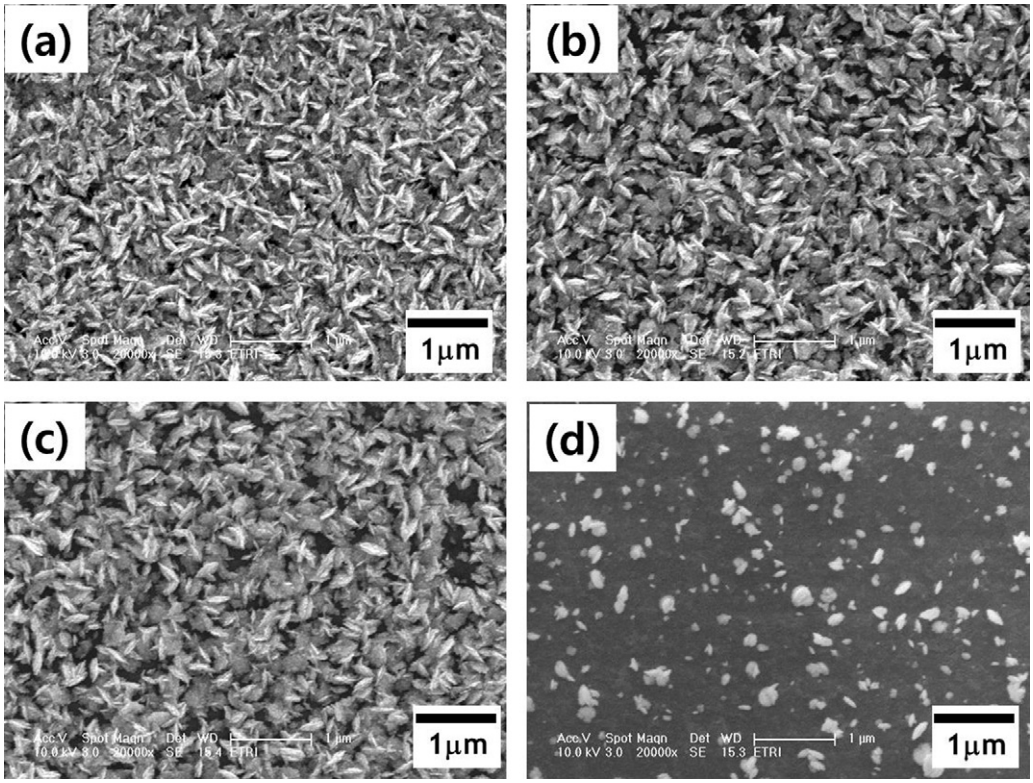

Fig. 2. Scanning electron microscope (SEM) images of the photodiode surface reacted with (a) 0 ppb, (b) 5 ppb, (c) 10 ppb, and (d) 15 ppb of Aflatoxin B1, and then silver-enhanced for 12 min.

AuNps, the photodiode surface was immersed in a 1:1 mixture of silver enhancer solution A and B (Product No. S5020 and S5145, Sigma–Aldrich) for 12 min, followed by rinsing in de-ionized water. During the silver enhancement step, silver atoms were deposited only on the AuNps, leading to the formation of opaque metal structures.

3.4. Electrical measurements of photoresponses

Photoresponses of a sensor chip were measured with a Hewlett-Packard 4156B Precision Semiconductor Parameter Analyzer, while the sensor chip was loaded on a probe station isolated within a metal dark box. As a light source for illuminating the photodiode area, a power-adjustable tungsten lamp of the probe station microscope was used. For varying concentration of Aflatoxin B1, the I_{DS} of the photodiode-driven p-MOSFET was measured at a drain-source bias (V_{DS}) of 500 mV, with the source of the p-MOSFET and the p+ contact of the photodiode commonly grounded. For a comparison of the photocurrent- and V_{OC}-based approaches, the photocurrent of photodiodes was also measured at a reverse-bias of 100 mV.

4. Results and discussion

Fig. 1c shows a typical dependence of the V_{OC} on the light power, for a 300 μm × 300 μm photodiode. As demonstrated in Fig. 1c, the V_{OC} of a Si photodiode increases abruptly just above the zero intensity, reaching ~0.3 V at a light power as low as 0.07 μW. Then, the V_{OC} keeps increasing with a decreasing rate, and is finally saturated at around 0.4 V. Such behavior is distinct from that of the photocurrent of a photodiode, which generally has a linear relationship with the light intensity (Budde, 1983). This observation implies that monitoring of the V_{OC} can provide a higher sensitivity with the light intensity near the dark point. By driving the gate of a p-MOSFET by the illuminated photodiode, the variation of V_{OC} could be transformed into that of the I_{DS}, as shown in Fig. 1c.

Usually, large-sized proteins with multiple epitopes can be detected by the sandwich-type immunoassay involving two kinds of antibodies, which provides a higher signal at a larger amount of the target molecule (Quinton et al., 2010). In our previous work (Ahn et al., 2010), the prostate specific antigen (PSA) (~33,000 Da) was also detected by the sandwich assay using similar silver-enhanced AuNP labels, but the PSA concentration was monitored from the photocurrent instead of the V_{OC}. In that case, as the fractional area of the screened region gradually increased with the PSA concentration (starting from zero) while maintaining a sufficiently low level across the concentration range of interest (0–50 ng/ml), the degradation of signal resolution occurring near the full coverage of enhanced particles was not a problem in achieving the sensitivity and working range as required for PSA (Ahn et al., 2010).

However, for small toxin molecules (<500 Da) having only one epitope, the sandwich assay is not applicable and the competitive assay using a single kind of antibodies is necessary (Sapsford et al., 2006; Lee et al., 2004; Ngundi et al., 2005). In this case, the coverage of metal particles is higher at a lower concentration of toxin molecules. Fig. 2 shows scanning electron microscope (SEM) images of the photodiode surface after a competitive reaction with 0, 5, 10, and 15 ppb of Aflatoxin B1, followed by silver-enhancement for 12 min. As expected, the coverage of opaque metal structures is highest in the absence of toxin molecules, and decreases as the toxin concentration increases.

In Fig. 2, it is remarkable that the coverage of enhanced AuNPs remains quite high (close to 100%) up to the toxin concentration of 10 ppb, but drops abruptly between 10 and 15 ppb. Consequently, while the toxin concentration increases from 0 to 10 ppb, the photocurrent remains as low as less than 1 μA showing a weak

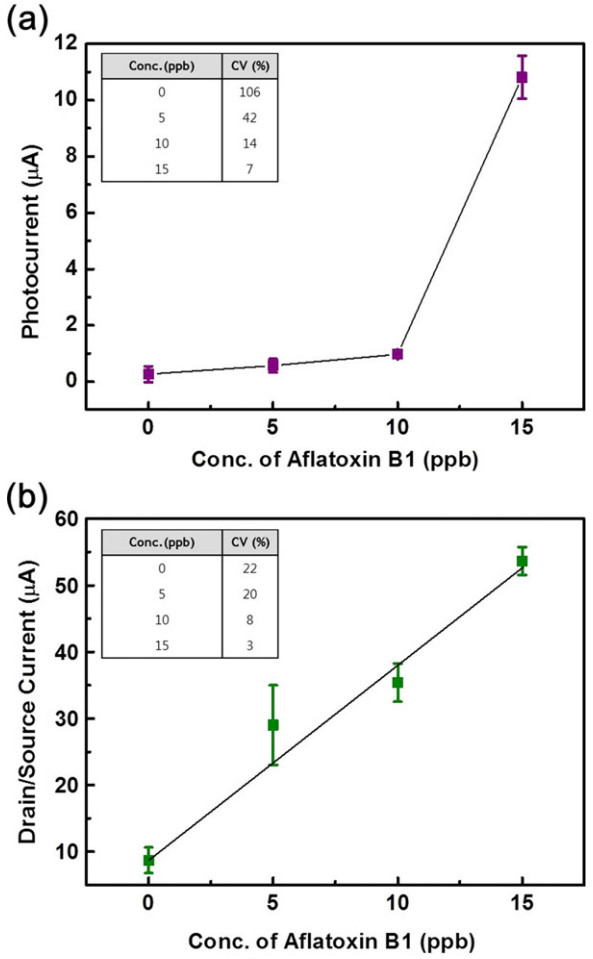

Fig. 3. Dependence of (a) the photocurrent of a 300 μm × 300 μm photodiode at a reverse-bias of 100 mV,and (b) the drain/source current (I_{DS}) of a photodiode-driven p-MOSFET at a drain-source bias (V_{DS}) of 500 mV, on the concentration of Aflatoxin B1 with the incident light power of 8.2 μW.The insets show the coefficient of variation (CV) for each data point obtained by averaging the data from five different sensor devices. The Pearson correlation coefficient for the data points in (b) is 0.983.

dependence on the toxin concentration (Fig. 3a). Above 10 ppb, however, the photocurrent begins to steeply increase and reaches 12 μA at 15 ppb. Such observation implies that, for a certain range of toxin concentration near zero point (with nearly 100% coverage of enhanced AuNPs), it is difficult to obtain any quantitative information using the photocurrent-based approach. By monitoring the photocurrent, only the 'on/off' evaluation referring to a cut-off level (10 ppb in the present case) is possible. According to the international standards for food safety, for Aflatoxin B1, it is crucial to achieve a quantitative analysis within the range of 0–15 ppb (Otsuki et al., 2001).

However, by monitoring the I_{DS} of a p-MOSFET driven by the V_{OC}, we could obtain a quantitative data curve for the toxin concentration ranged from 0 to 15 ppb. Fig. 3b shows the variation of I_{DS} with the toxin concentration. In Fig. 3b, as the toxin concentration increases from 0 to 15 ppb, the I_{DS} also increases linearly by about 6 times, providing a sufficiently large output change (10–20 μA) for the interval of 5 ppb. Such enhancement of signal resolution at low toxin concentrations can be attributed to the abrupt (and non-linear) variation of the V_{OC} with the light intensity, as shown in Fig. 1c. These results demonstrate that, if we monitor the V_{OC} (i.e., I_{DS}) instead of the photocurrent, a high sensitive and quantitative detection of small toxin molecules is also possible using the photodiode sensor.

Previously, optical sensing methods utilizing fluorescence labels have been most widely used for detecting small toxin molecules (Sapsford et al., 2006; Lee et al., 2004; Ngundi et al., 2005; Wang and Wang, 2008), but the need for large and expensive optical instruments is still a barrier in developing portable sensing systems for the point-of-use (Wang et al., 2007). As an alternative candidate for overcoming such limitation of optical sensing techniques, FET-type biosensors may also be considered, where the electrical signal outputs allow the miniaturization of signal readout and data processing modules using the CMOS integrated circuit technology (Kim et al., 2007, 2010; Nakazato, 2009). However, in FET-type biosensors, the channel current is also affected by the ionic strength or pH of the sample solution, which makes it hard to obtain reproducible signal outputs (Kim et al., 2010; Park et al., 2011). In addition, as the electrical measurement has to be performed in an aqueous solution environment, it still remains challenging to avoid the current leakage or device degradation for maintaining high device stability (Tian et al., 2011).

With all these considerations, the scheme of photosensitive biosensors using metallic nanoparticle labels can be regarded as the combination of advantages of both the optical and FET-based approaches. By utilizing optical input signals, the photosensitive sensor allows highly stable and reproducible measurement with no interference due to pH change, salinity, or external electrical noises (Ahn et al., 2010; Li et al., 2005; Wang et al., 2007). At the same time, as the output signals are fully electronic, the photosensitive sensor can eliminate the need for bulky optical instrumentations, enabling the development of low-cost and portable systems (or devices) with the whole circuitry for signal readout and data processing integrated on a single platform (Ahn et al., 2010; Li et al., 2005; Wang et al., 2007). Combined with the new sensing scheme based on the variation of V_{OC} as proposed, the CMOS compatible photosensitive biosensor can be utilized as a powerful tool for high-sensitive, simple, and low-cost detection of mycotoxins, targeting the point-of-use applications for food industry.

5. Conclusions

We developed a new type of photosensitive biosensor with a CMOS compatible Si photodiode integrated circuit, which enables the high-sensitive detection of small mycotoxin molecules requiring a competitive assay. By employing AuNPs as labels to generate opaque metal networks on a photodiode surface and monitoring the V_{OC} instead of the photocurrent, we could achieve a high signal resolution at low concentrations even with the competitive assay, which is owing to the abrupt and non-linear change of V_{OC} with the light intensity under nearly dark conditions. Utilizing optical input and electrical output signals, the new V_{OC}-based photosensitive biosensor provides a useful tool for high-sensitive and low-cost detection of mycotoxins, which can contribute to the development of point-of-use applications for food safety.

Acknowledgements

This work was supported by the Ministry of Knowledge Economy in Korea [2009-F-008-01, Programmable Bio-CMOS Field Effect Transistors]. The authors would like to thank Miss Cho Hee Lee for her technical supports.

References

Ahn, C.-G., Ah, C.S., Kim, T.-Y., Park, C.W., Yang, J.-H., Kim, A., Sung, G.Y., 2010. Appl. Phys. Lett. 97, 103703.
Budde, W., 1983. Appl. Opt. 22 (11), 1780–1784.
Kim, A., Ah, C.S., Yu, H.Y., Yang, J.-H., Baek, I.-B., Ahn, C.-G., Park, C.W., Jun, M.S., Lee, S., 2007. Appl. Phys. Lett. 91, 103931.
Kim, A., Ah, C.S., Park, C.W., Yang, J.-H., Kim, T., Ahn, C.-G., Park, S.H., Sung, G.Y., 2010. Biosens. Bioelectron. 25, 1767–1773.
Lee, N.A., Wang, S., Allan, R.D., Kennedy, I.R., 2004. J. Agric. Food Chem. 52, 2746–2755.
Li, J., Xu, C., Zhang, Z., Wang, Y., Peng, H., Lu, Z., Chan, M., 2005. Sens. Actuators B: Chem. 106, 378–382.
Nakazato, K., 2009. Sensors 9, 8831–8851.
Ngundi, M.M., Shriver-Lake, L.C., Moore, M.H., Lassman, M.E., Ligler, F.S., Taitt, C.R., 2005. Anal. Chem. 77, 148–154.
Otsuki, T., Wilson, J.S., Sewadeh, M., 2001. Eur. Rev. Agric. Econ. 28 (2), 263–283.
Park, C.W., Ah, C.S., Ahn, C.-G., Yang, J.-H., Kim, A., Kim, T.-Y., Sung, G.Y., 2011. Sens. Actuators B: Chem. 154, 164–168.
Quinton, J., Charruault, L., Nevers, M.-C., Volland, H., Dognon, J.-P., Créminon, C., Taran, F., 2010. Anal. Chem. 82, 2536–2540.
Sapsford, K.E., Taitt, C.R., Fertig, S., Moore, M.H., Lassman, M.E., Maragos, C.M., Shriver-Lake, L.C., 2006. Biosens. Bioelectron. 21, 2298–2305.
Tian, R., Regonda, S., Gao, J., Liu, Y., Hu, W., 2011. Lab Chip 11, 1952–1961.
Wang, X.-H., Wang, S., 2008. Sensors 8, 6045–6054.
Wang, Y., Xu, C., Li, J., He, J., Chan, M., 2007. IEEE Trans. Electron. Devices 54 (6), 1549–1554.